World Academy of Science, Engineering and Technology
International Journal of Biomedical and Biological Engineering
Vol:3, No:6, 2009

Action Potential Propagation in Inhomogeneous 2D Mouse Ventricular Tissue Model

Vladimir E. Bondarenko and Randall L. Rasmusson

***Abstract*—** Heterogeneous repolarization causes dispersion of the T-wave and has been linked to arrhythmogenesis. Such heterogeneities appear due to differential expression of ionic currents in different regions of the heart, both in healthy and diseased animals and humans. Mice are important animals for the study of heart diseases because of the ability to create transgenic animals. We used our previously reported model of mouse ventricular myocytes to develop 2D mouse ventricular tissue model consisting of 14,000 cells (apical or septal ventricular myocytes) and to study the stability of action potential propagation and Ca^{2+} dynamics. The 2D tissue model was implemented as a FORTRAN program code for high-performance multiprocessor computers that runs on 36 processors. Our tissue model is able to simulate heterogeneities not only in action potential repolarization, but also heterogeneities in intracellular Ca^{2+} transients. The multicellular model reproduced experimentally observed velocities of action potential propagation and demonstrated the importance of incorporation of realistic Ca^{2+} dynamics for action potential propagation. The simulations show that relatively sharp gradients of repolarization are predicted to exist in 2D mouse tissue models, and they are primarily determined by the cellular properties of ventricular myocytes. Abrupt local gradients of channel expression can cause alternans at longer pacing basic cycle lengths than gradual changes, and development of alternans depends on the site of stimulation.

***Keywords*—**Mouse, cardiac myocytes, computer simulation, action potential.

I. Introduction

THE cardiac action potential (AP) arises at a cellular level from interaction of several currents to produce a rapid upstroke and relatively slower repolarization phase. While the action potential upstroke is dominated by the behavior of the sodium channel, repolarization results from a complex interaction of multiple inward and outward currents [1]-[4]. This complex process of repolarization returns the myocyte to its resting potential and also determines calcium dynamics and the strength and duration of cardiac muscle contraction. The complex and indirect interactions between multiple current systems can make intuitive predictions concerning repolarization behavior nearly impossible. Therefore, the study of cardiac cellular repolarization has a long history of the use of computer models to make and test predictions concerning the ionic basis of repolarization behavior (for reviews see [5]-[7]).

The theoretical study of the systems biology of repolarization has also been augmented by the development of transgenic animals, primarily the mouse, in which the consequences of specific mutations can be examined in the context of a functional mammalian cardiac environment [8]. We recently published a cellular model of the mouse left ventricular and septal action potentials that can also be used in relating changes in ion channel expression to changes in action potential behavior [4]. Bridging the gap between cellular behavior and behavior of the multicellular system that constitutes the ventricle and/or whole heart has raised questions about the appropriateness of the mouse heart for studying questions of spatial heterogeneity of repolarization [9], [10]. The mouse heart, with its small size and small number of cells means that propagation through physiologically relevant numbers of cells can be accomplished without cellular model simplification or the use of continuum equation approximations. In this paper we test the ability of a complete cellular model of the mouse to sustain physiologically relevant spatial gradients of repolarization.

There are several experimental results from transgenic mouse hearts and mouse hearts that have been modified pharmacologically [11]-[13]. They suggest that molecular heterogeneity of currents produces significant spatial heterogeneity and/or dispersion of repolarization. In order to examine this problem, we employed a comprehensive model of the mouse cardiac cell with discrete gap junctions and simplified geometries to examine the ability of molecular heterogeneity to change the spatial variation of repolarization. We developed a 2D model of the ventricular mouse cardiac tissue, consisting of 14,000 cardiac myocytes, with propagation velocities and characteristics of AP repolarization matched to those measured by Gutstein *et al.* [14]. Our simulations predict that substantial gradients in repolarization and intracellular $[Ca^{2+}]_i$ transients can be maintained through heterogeneity of expression of ion channel currents in distances of about ten cells. While electrotonic interactions caused modification of the AP, such modifications did not eliminate heterogeneity of repolarization. We also found that abrupt changes in cardiac channel expression can cause instability of intracellular Ca^{2+} transients that demonstrate

This work was supported in part by a grant from the NIH 5R01HL062465 to R. L. Rasmusson and startup fund from the Georgia State University to V. E. Bondarenko.

V. E. Bondarenko is with the Department of Mathematics and Statistics, Georgia State University, Atlanta, GA 30303 USA (corresponding author, phone: 404-413-6440; fax: 404-413-6403; e-mail: matvxb@langate.gsu.edu).

R. L. Rasmusson is with the Department Physiology and Biophysics, University of Buffalo, SUNY, Buffalo, NY 14214 USA (e-mail: rr32@buffalo.edu).

alternating small- and large-amplitude transients. These results suggest that the mouse heart may be a suitable model for the study of heterogeneous channel expression.

II. Methods

We used our previously published model of mouse ventricular myocytes for 2D tissue model development (Fig. 1). The model parameters are the same as in [4] for apical and septal cells. Each model myocyte is described by the equations from [4] with corresponding initial conditions plus intercellular currents:

$$\frac{dV_i}{dt} = -\frac{1}{C_{m,i}}\left(I_{memb,i} - I_{stim,i} + I_{gap,i}\right), \quad i = 1, \ldots, N \qquad (1)$$

Here i is the cell number, $C_{m,i}$ is the membrane capacitance of the *i*th cell, V_i is the membrane potential, $I_{memb,i}$ is the total membrane ion current [4], $I_{stim,i}$ is the stimulus current, $I_{gap,i}$ is the gap current [15].

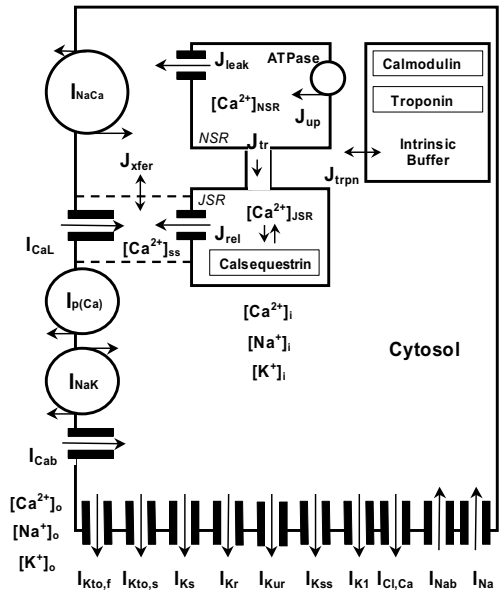

Fig. 1. Schematic diagram of the mouse model ionic currents and Ca^{2+} fluxes. Transmembrane currents are: I_{Na}, the fast Na^+ current, I_{CaL}, the L-type Ca^{2+} current, $I_{p(Ca)}$, the Ca^{2+} pump, I_{NaCa}, the Na^+-Ca^{2+} exchanger, $I_{Kto,f}$, the rapid transient outward K^+ current, $I_{Kto,s}$, the slow transient outward K^+ current, I_{Kr}, the rapid delayed-rectifier K^+ current (mERG), I_{Kur}, the ultra-rapid delayed-rectifier K^+ current, I_{Kss}, the steady-state non-inactivating K^+ current, I_{K1}, the time-independent K^+ current, I_{Ks}, the slow delayed-rectifier K^+ current, I_{NaK}, the Na^+-K^+ pump, and I_{Cab} and I_{Nab}, the Ca^{2+} and Na^+ background currents. I_{stim} is the external stimulation current. The Ca^{2+} fluxes within the cell are: J_{up}, uptake Ca^{2+} from the cytosol to the network sarcoplasmic reticulum (SR), J_{rel}, Ca^{2+} release from the junctional SR, J_{tr}, Ca^{2+} flux from the network to junctional SR, J_{leak}, Ca^{2+} leak from the SR to the cytosol, J_{xfer}, Ca^{2+} flux from the subspace volume to the bulk myoplasm, J_{trpn}, Ca^{2+} flux to troponin. The model includes Ca^{2+} buffering by troponin and calmodulin in the cytosol and by calsequestrin in the SR. Modified from [4].

The 2D model tissue consisted of 14,000 mouse ventricular myocytes formed into a rectangular sheet of 200 myocytes × 70 myocytes (n_x = N = 200, n_y = L = 70, Fig. 2). The number of cells and dimensions of 2D tissue were chosen from the experimental data of Fig. 4A from [16] to match the reported surface of the mouse ventricle of about 7.0 mm × 7.0 mm. This approximation is based on an approximate cell length of 100 μm and a cell width 35 μm [1], [17], [18]. The area of the simulated surface also approximated about 1/3 of the whole mouse ventricle [10]. Each myocyte in 2D model is described by (1) however with different equations for gap junctional resistances to account for anisotropic propagation. The formulation used was: $I_{gap,i} = g_{gap,xi}(-V_{i-1} + 2V_i - V_{i+1}) + g_{gap,yi}(-V_{i-nx} + 2V_i - V_{i+nx})$, where $g_{gap,xi}$ and $g_{gap,yi}$ are the gap conductances along axes X and Y of the rectangle, respectively. Note that for the myocytes on the tissue perimeter the boundary conditions are required, and the expression for $I_{gap,i}$ contains only 2 or 3 intercellular currents from the neighboring cells. We used values of $g_{gap,xi} = g_{gap,x}$ and $g_{gap,yi} = g_{gap,y}$ for all myocytes that were varied from 1 to 80 nS/pF. The amplitude of the stimulus current, $I_{stim,i}$, was varied from 180 to 2000 pA/pF to be equal approximately to 150% of the threshold value, depending on the intercellular conductance. In all cases, the stimulus pulse duration was equal to 0.5 ms. Details of the stimulation protocols are described in the text or figure legends.

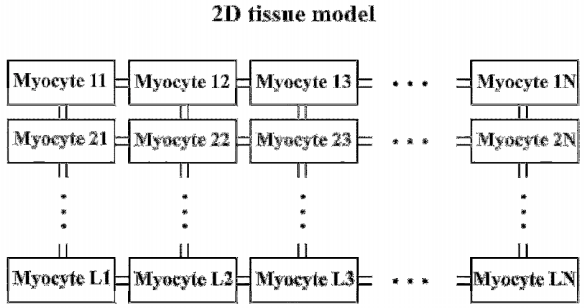

Fig. 2. Schematic diagram of 2D mouse cardiac tissue model.

Model equations (1) were solved using a fourth-order Runge-Kutta method with a time step of 0.0001 ms. The resting values of state variables of the model myocytes were used as the initial conditions in our simulations. In the inhomogeneous case all cells were in equilibrium before stimulation. Simulations of 2D model were performed using 36 processors (3.2 GHz Intel Xeon "Irwindale") of a Dell Linux Cluster. One processor was used for data input-output and the remaining 35 processors performed numerical simulations, 400 model myocytes on each processor.

III. Results

The experimentally measured propagation velocity of AP in mouse heart tissues depends on the direction of propagation and intercellular coupling [14], [16], [19], [20]. We performed simulations of AP propagation in 2D model of the mouse tissue. Fig. 3 shows snapshots of the distribution of membrane potential at two different intercellular couplings $g_{gap,y}$ = 80 and 5 nS/pF ($g_{gap,x}$ = 50 nS/pF for both simulations) and at two

time moments, 11 and 15 ms, in the homogeneous tissue consisting of the apical cells (similar results were obtained for septal tissue). For relatively large intercellular coupling with $g_{gap,y}$ = 80 nS/pF, the AP front creates an extensive depolarized region of about 30 myocytes ahead of the peak of AP within 1 ms after the stimulus is applied (Fig. 3A), while at the smaller coupling $g_{gap,y}$ = 5 nS/pF this region is only about 8 myocytes in length (Fig. 3C). Five milliseconds later after the stimulus, the AP occupies almost the whole tissue at $g_{gap,y}$ = 80 nS/pF (Fig. 3B) and only a fraction of the tissue at $g_{gap,y}$ = 5 nS/pF (Fig. 3D). This simulation shows that the whole tissue may become unexcitable during normal AP propagation. On the other hand, uncoupled tissue can easily be excited by a premature or ill-timed random stimulus and effect AP propagation and potentially be very pro-arrhythmic. This is consistent with experimental evidence which showed that slower conductance in the mouse heart is pro-arrhythmic when there is reduced intercellular coupling [14], [19].

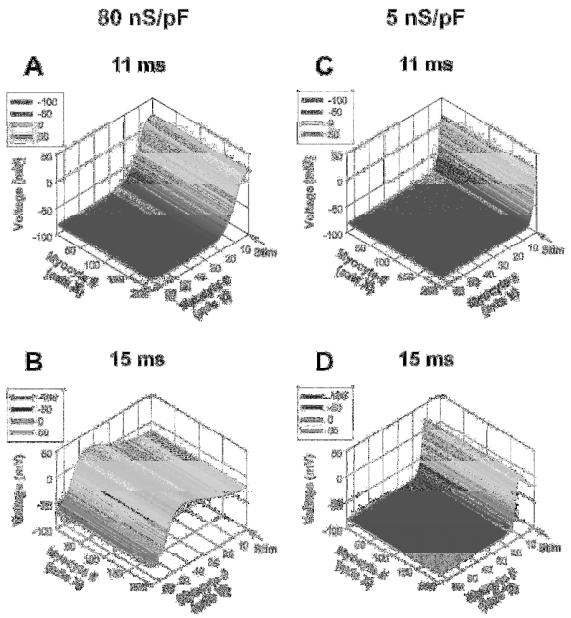

Fig. 3. Action potential propagation in a 2D model of the mouse uniform multicellular cardiac tissue: dependence on intercellular coupling along axis Y, $g_{gap,y}$ ($g_{gap,x}$ = 50 nS/pF). 14,000 model apical myocytes form a 2D rectangular surface (200 myocytes and 70 myocytes along axes X and Y, respectively). Stimulus current was applied to row 1 at 10 ms (I_{stim} = 2000 pA/pF, τ_{stim} = 0.5 ms). Panels A and B show snapshots at 11 and 15 ms, respectively, for $g_{gap,y}$ = 80 nS/pF; Panels C and D show snapshots at 11 and 15 ms, respectively, for $g_{gap,y}$ = 5 nS/pF. Note the substantial differences in AP propagation velocities.

We validated the independence of propagation velocities on the stimulus number and checked for potential effects of non-steady-state conditions in homogeneous 2D tissue by comparing propagation velocities for the APs initiated by the 1st and 10th stimuli. The results do not show substantial differences. We also found the values of $g_{gap,x}$ = 75 and $g_{gap,y}$ = 25 nS/pF that correspond to the experimental minimum and maximum propagation velocities in orthogonal directions (shown by solid and dashed horizontal lines in Fig. 4, 0.38 and 0.62 m/s, respectively [14]).

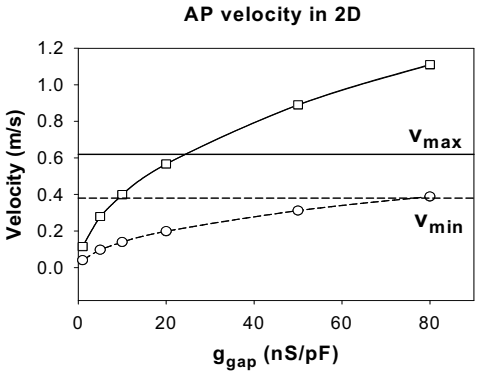

Fig. 4. Velocity of the action potential propagation in 2D model of the mouse multicellular cardiac tissue as functions of intercellular coupling $g_{gap,x}$ and $g_{gap,y}$. Filled and unfilled symbols (they completely overlap) plot AP velocities induced by the 1st stimulus in the tissues consisting of the apical and septal cells, respectively. Squares and circles correspond to the longitudinal and transverse AP propagation velocities. Solid and dashed horizontal lines show experimental velocities v_{max} and v_{min} measured by Gutstein *et al.* [14].

We also studied the effects of an abrupt inhomogeneity in cellular type on AP repolarization and $[Ca^{2+}]_i$ transients in 2D model tissues (Fig. 5). Inhomogeneous 2D tissue consists of 7,000 (35 rows) septal and 7,000 (35 rows) apical cells and is uniform in the X axis direction. Intercellular conductances were set to $g_{gap,x}$ = 75 nS/pF and $g_{gap,y}$ = 25 nS/pF to match experimental values of AP propagation velocity [14]. The stimulus current was applied either to row 1 or to row 70. These simulations showed an unexpected asymmetry in AP propagation and in the properties of $[Ca^{2+}]_i$ transients (Fig. 5). Figs. 5A and 5D show snapshots of membrane potential in inhomogeneous 2D tissue at 20 ms when stimulated from rows 1 and 70, respectively. The AP waveform has a well-defined inflection in its spatial distribution at the boundary between myocyte types when stimulated from the septum region (Fig. 5A). However, when the tissue was stimulated from the apex region, the AP waveform did not have the same inflection (Fig. 5D). Different sites of stimulation also resulted in different magnitudes of $[Ca^{2+}]_i$ transients, with a larger peak $[Ca^{2+}]_i$ during stimulation from the apex region (Figs. 5B and 5E). The gradient of the $[Ca^{2+}]_i$ transients also persisted for a longer time when the stimulus was applied from the apex region (Figs. 5C and 5F).

Inhomogeneities in AP repolarization in 2D tissue result from an interaction of cellular mechanisms of AP generation and electrotonic currents (Fig. 6). During the AP upstroke, electrotonic currents effectively decrease AP overshoot. APD_{25} is mainly determined by the cellular ionic currents and shows a clear heterogeneity in repolarization between the septal and apical cells, with small transition region of about

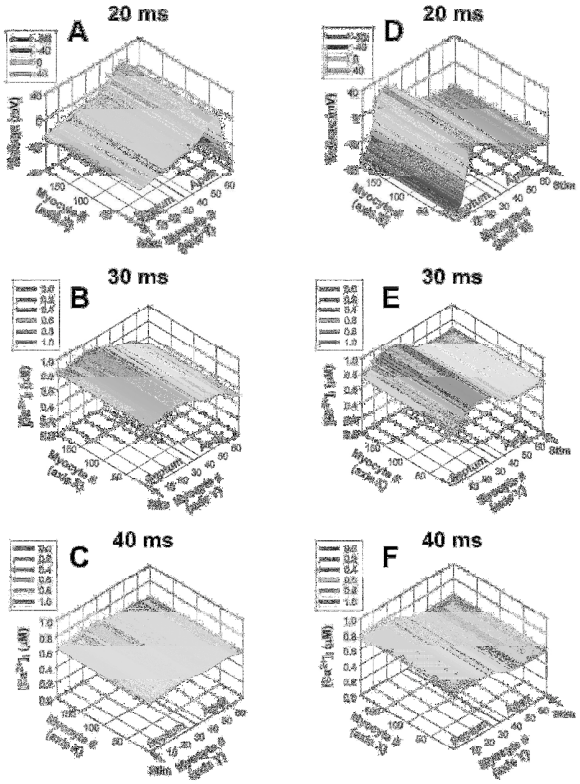

Fig. 5. Action potential propagation (Panels A and D) and intracellular Ca^{2+} transients, $[Ca^{2+}]_i$, (Panels B, C, E, and F) for 2D model of the mouse inhomogeneous multicellular cardiac tissue. 14,000 model apical myocytes form 2D rectangular surface (200 myocytes and 70 myocytes along axes X and Y, respectively; $g_{gap,x}$ = 75 nS/pF and $g_{gap,y}$ = 25 nS/pF). Inhomogeneous tissues consisted of 35 rows of septal (rows 1-35) and 35 rows of apical (rows 36-70) myocytes. The stimulus current was applied to row 1 (Panels A-C) or to row 70 (Panels D-F) at 10 ms (I_{stim} = 900 pA/pF, τ_{stim} = 0.5 ms). Panels A and D show snapshots of AP at 20 ms; Panels B and E show snapshots of $[Ca^{2+}]_i$ at 30 ms; Panels C and F show $[Ca^{2+}]_i$ at 40 ms. Note that the inhomogeneities of $[Ca^{2+}]_i$ were more persistent when stimulation was applied to apical cells (Panels E and F).

10 rows of myocytes at the boundary between the cells of different types, and some boundary condition artifacts at the ends of 2D tissue (solid and dotted lines in Fig. 6A). 2D tissue with linear dependence of conductivities for important K^+ currents ($I_{Kto,f}$, $I_{Kto,s}$, I_{Kur}, and I_{Kss}) from the septal to apical values also demonstrated a linear dependence of APD_{25} on the row number (dashed and dot-dashed lines in Fig. 6A). Small-dashed and dash-dot-dot lines in Fig. 6A show corresponding APD_{25} for uniform 2D tissue models consisting of the septal or apical cells. The picture of AP repolarization becomes more complex for APD_{50} for 2D tissue with abrupt transition region between myocyte types (Fig. 6B). The transition regions at the boundary between myocyte types for APD_{50} are shifted towards the sites of stimulation (solid and dotted lines in Fig. 6B). Finally, the APD_{75} is a linear function of the row number and demonstrates the substantial dependence of APD_{75} on the site of stimulation, with the longer values at the site of stimulation (Fig. 6C).

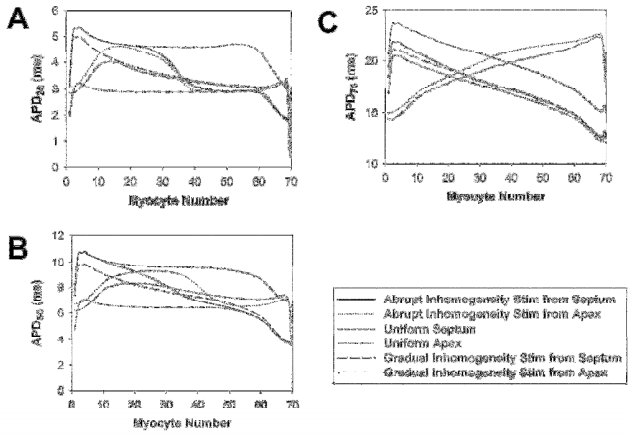

Fig. 6. Action potential duration in a 2D model of the mouse tissue with inhomogeneous and homogeneous cellular phenotypes. Panels A, B, and C show APD_{25}, APD_{50}, and APD_{75}, respectively. Solid and dotted lines show APDs for inhomogeneous model with 35 rows of septal (rows 1-35) and 35 rows of apical (rows 36-70) myocytes, with stimulation from the rows 1 and 70, respectively; short dashed and dash-dot-dot lines plot APDs for a uniform tissue model consisting of the septal or apical cells, respectively, with stimulation of row 1; long dashed and dash-dot lines show APDs for inhomogeneous tissue model stimulated from rows 1 and 70, respectively, with linear dependencies of conductivities for the dominant repolarizing K^+ currents ($I_{Kto,f}$, $I_{Kto,s}$, I_{Kur}, and I_{Kss}) between typical septal cells (row 1) and typical apical cell (row 70). Panels A and B show that APD_{25} and APD_{50} were determined primarily by the cell type (septal or apical), excluding artifacts at the boundaries of the tissue and at the sites of stimulation. In turn, APD_{75} depended substantially on the site of stimulation and was determined primarily by electrotonic interactions (Panel C). In all simulations for this figure, the stimulus current (I_{stim} = 900 pA/pF, τ_{stim} = 0.5 ms) was applied at 10 ms; $g_{gap,x}$ = 75 nS/pF and $g_{gap,y}$ = 25 nS/pF.

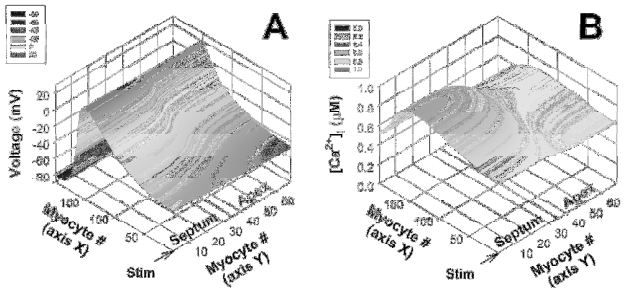

Fig. 7. Transmural heterogeneity of repolarization in 2D model of the mouse inhomogeneous multicellular cardiac tissues. Action potential (Panel A) and intracellular calcium transients, $[Ca^{2+}]_i$, (Panel B). Inhomogeneous tissue model is the same as in Fig. 5. However, stimulus current is applied to column 1 at 10 ms (I_{stim} = 900 pA/pF, t_{stim} = 0.5 ms). Panel A shows snapshot of AP at time moment 25 ms; Panel B shows snapshot of $[Ca^{2+}]_i$ at time moment 35 ms. Note transmural inhomogeneities of both AP and $[Ca^{2+}]_i$ transients on scale of about 10 myocytes.

In order to verify whether inhomogeneities in repolarization sustain during transverse AP propagation, we also stimulated column 1 of the abrupt inhomogeneous 2D tissue (Fig. 7). In this case, the front of AP propagation was in the transverse direction to the division line between the two myocyte types. As it is seen from Fig. 7A, there is only a narrow region on the boundary between the apical and the septal myocytes where the AP changes from longer to shorter duration. The differences in AP duration between the cell types determine the differences in intracellular $[Ca^{2+}]_i$ transients (Fig. 7B). They considerably larger for septal than for apical myocytes, and the transition region is determined by the scale where AP duration varies.

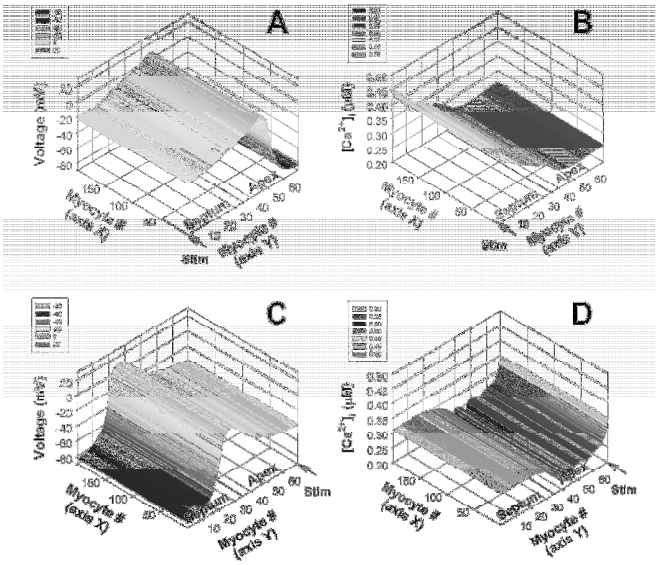

Fig. 8. Action potential propagation in 2D model of the mouse inhomogeneous multicellular cardiac tissues. Action potential (Panels A and C) and intracellular calcium transients, $[Ca^{2+}]_i$, (Panels B and D). Inhomogeneous tissue model is the same as in Fig. 5. Stimuli are applied to row 1 (Panels A and B) or to row 70 (Panels C and D) with basic cycle length 80 ms (I_{stim} = 900 pA/pF, τ_{stim} = 0.5 ms). Panels A and C show snapshots of the 27th AP at time moment 10 ms after the stimulus; Panels B and D show snapshots of the corresponding $[Ca^{2+}]_i$. Note inhomogeneities of $[Ca^{2+}]_i$ transients (alternans) when stimuli are applied from the apex (Panels D).

The physical arrangement that was most susceptible to alternans was the 2D abruptly inhomogeneous tissue model stimulated from the apical region (Fig. 8). Pacing of abrupt inhomogeneous 2D tissue from the septum region (Figs. 8A and 8B) with basic cycle length 80 ms does not produce alternans. When stimulation is applied to the apex region, the threshold for alternans appearance was 82 ms. An example of simulations of AP and $[Ca^{2+}]_i$ transients in this 2D tissue at pacing with basic cycle length 80 ms is shown in Figs. 8C and 8D. Initially, the alternans starts from the abrupt transition region where the septum myocytes adjoin the apex cells and then spreads, mostly towards the region of the tissue containing model apex cells (Fig. 8D). The alternans is discordant, with small and large $[Ca^{2+}]_i$ transients in different regions of the column oscillating in opposite phases. These simulation data suggest a destabilizing role of the abrupt gradient of myocyte type together with the site of stimulation (the apex region).

IV. Discussion

Ventricular arrhythmias and sudden cardiac death are a major source of morbidity and mortality in Western Hemisphere [21]. Many sudden cardiac deaths occur in patients with no prior history of heart disease, and often without evidence of significant coronary artery disease or myocardial infarction [21]. A few of these cases may reflect the relatively rare genetically-inherited disorders such as the various forms of long QT syndrome [22], [23]. However, the majority are likely the result of electrical remodeling associated with the different stages of silent ischemic heart disease. In the absence of morphological changes, altered cellular electrical function is likely to be the primary mechanism of such arrhythmias.

Arrhythmias are not simply cellular events, but are abnormal patterns of electrical behavior that involve wave movement through multicellular tissue. These waves, or reentrant arrhythmias, have been a frequent subject of mathematical investigation [24]-[37]. The generation of spiral waves and their degeneration into chaotic behavior has been accepted as a mechanism of pathophysiological conditions such as tachycardia and fibrillation [38]-[46]. As such, they have been largely modeled using simplified FitzHugh-Nagumo formulations [47]-[50]. This approach can explain how such processes may result from an appropriately-timed premature stimulus [51]-[54].

Recently two other models of mouse ventricular myocytes were developed and simulations of AP propagation in mouse ventricular cardiac tissues were performed [10], [55]. In general, such simulations have neglected or greatly simplified calcium handling despite its well established importance in arrhythmias [46]. However, the models were able to simulate some properties of AP repolarization and propagation. Sampson and Henriquez [10] simulated AP propagation in anatomically detailed heterogeneous model of the mouse ventricle. Relative to our findings their model overestimates the influence of electrotonic interactions at early stages of repolarization, but their results are similar to ours for later stages of repolarization, where the gradient of repolarization is significantly affected by electrotonic interactions. Noujaim *et al.* [55] studied mechanism of re-entry in 2D mouse ventricular model tissue for explanation of experimentally observed arrhythmias in the mouse heart. They found that the rotor in wild type 1 cm × 1 cm 2D tissue is terminated after about two rotations. In contrast, a rotor in the same size tissue, but with the model ventricular myocytes for transgenic mice overexpressing I_{K1}, sustained re-entry.

Our simulations demonstrated that heterogeneities in K^+ channel expression can cause instability in the mouse ventricle, such as Ca^{2+} alternans, at rapid pacing. This instability can also exist in homogeneous apical tissue, but at shorter basic cycling lengths. Comparing the two results shows that the abrupt inhomogeneity in cardiac channel

expression can provoke instability of Ca^{2+} dynamics resulting in Ca^{2+} alternans.

Although some quantitative details of AP repolarization and propagation may differ between species, the experimental evidence from mouse hearts is that they provide a good model for relating cellular and molecular mechanisms to whole heart function. For example, it has long been proposed that there is a complex interaction between K^+ channels and Ca^{2+} handling. Myocytes from transgenic Kv1.4 ($I_{Kto,s}$) knock-out mice with an additional dominant-negative mutation in Kv4.2 ($I_{Kto,f}$), have markedly prolonged APDs [56]. Some cells even exhibit EADs, which were not present in wild type or single mutant Kv4.2[W362F] cells [56]. The smaller K^+ currents at repolarized potentials prolong the APD and increase Ca^{2+} influx into the myocyte as well as limit the amount of K^+ current during the "vulnerable window".

Thus, our 2D model of mouse ventricular tissue is able to simulate interactions between repolarization currents and Ca^{2+} dynamics. The model demonstrated that despite the small mouse heart, the heterogeneities of repolarization and $[Ca^{2+}]_i$ transients can be sustained on the small scale of about 10 cells. Such heterogeneities are important for stability AP propagation and Ca^{2+} dynamics and they increase susceptibility ventricular tissue to Ca^{2+} alternans.

REFERENCES

[1] C. H. Luo and Y. Rudy, "A dynamic model of the cardiac ventricular action potential. I. Simulations of ionic currents and concentration changes," *Circ. Res.*, vol. 74, pp. 1071-1096, Jun. 1994.

[2] M. S. Jafri, J. J. Rice, and R. L. Winslow, "Cardiac Ca^{2+} dynamics: the roles of ryanodine receptor adaptation and sarcoplasmic reticulum load," *Biophys. J.,* vol. 74, pp. 1149-1168, Mar. 1998.

[3] S. V. Pandit, R. B. Clark, W. R. Giles, and S. S. Demir, "A mathematical model of action potential heterogeneity in adult rat left ventricular myocytes," *Biophys. J.,* vol. 81, pp. 3029-3051, Dec. 2001.

[4] V. E. Bondarenko, G. P. Szigeti, G. C. L. Bett, S.-J. Kim, and R. L. Rasmusson, "Computer model of action potential of mouse ventricular myocytes," *Am. J. Physiol.,* vol. 287, pp. H1378-H1403, Sep. 2004.

[5] D. Noble and Y. Rudy, "Models of cardiac ventricular action potentials: iterative interaction between experiment and simulation," *Phil. Trans. R. Soc. Lond. A,* vol. 359, pp. 1127-1142, Jun. 2001.

[6] J. L. Puglisi, F. Wang, and D. M. Bers, "Modeling the isolated cardiac myocyte," *Prog. Biophys. Mol. Biol.,* vol. 85, pp. 163-178, Jun.-Jul. 2004.

[7] Y. Rudy and J. R. Silva, "Computational biology in the study of cardiac ion channels and cell electrophysiology," *Q. Rev. Biophys.,* vol. 39, pp. 57-116, Feb. 2006.

[8] J. M. Nerbonne, C. G. Nichols, T. L. Schwarz, and D. Escande, "Genetic manipulation of cardiac K^+ channel function in mice: what have we learned, and where do we go from here?" *Circ. Res.,* vol. 89, pp. 944-956, Nov. 2001.

[9] C. S. Henriquez, J. V. Tranquillo, D. Weinstein, E. W. Hsu, and C. R. Johnson, "Three-dimensional propagation in mathematic models: Integrative model of the mouse heart," in *Cardiac Electrophysiology: From Cell to Bedside*, 4th ed., D. P. Zipes and J. Jalife, Eds. Philadelphia, PA: Saunders, 2004, pp. 273-281.

[10] K. J. Sampson and C. S. Henriquez, "Electrotonic influences on action potential duration dispersion in small hearts: a simulation study," *Am. J. Physiol.,* vol. 289, pp. H350-H360, Jul. 2005.

[11] L. C. Baker, B. London, B.-R. Choi, G. Koren, and G. Salama, "Enhanced dispersion of repolarization and refractoriness in transgenic mouse hearts promotes reentrant ventricular tachycardia," *Circ. Res.,* vol. 86, pp. 396-407, Mar. 2000.

[12] B. C. Knollmann, A. N. Katchman, and M. R. Franz, "Monophasic action potential recordings from intact mouse heart: validation, regional heterogeneity, and relation to refractoriness," *J. Cardiovasc. Electrophysiol.,* vol. 12, pp. 1286-1294, Nov. 2001.

[13] L. C. Baker, R. Wolk, B.-R. Choi, S. Watkins, P. Plan, A. Shah, and G. Salama, "Effects of mechanical uncouplers, diacetyl monoxime, and cytochalasin-D on the electrophysiology of perfused mouse hearts," *Am. J. Physiol.,* vol. 287, pp. H1771-H1779, Oct. 2004.

[14] D. E. Gutstein, G. E. Morley, H. Tamaddon, D. Vaidya, M. D. Schneider, J. Chen, K. R. Chien, H. Stuhlmann, and G. I. Fishman, "Conduction slowing and sudden arrhythmic death in mice with cardiac-restricted inactivation of connexin43," *Circ. Res.,* vol. 88, pp. 333-339, Feb. 2001.

[15] T. R. Chay, "Proarrhythmic and antiarrhythmic actions of ion channel blockers on arrhythmias in the heart: model study," *Am. J. Physiol.,* vol. 271, pp. H329-H356, Jul. 1996.

[16] D. Vaidya, G. E. Morley, F. H. Samie, and J. Jalife, "Reentry and fibrillation in the mouse heart. A challenge to the critical mass hypothesis," *Circ. Res.,* vol. 85, pp. 174-181, Jul. 1999.

[17] R. B. Clark, A. Tremblay, P. Melnyk, B. G. Allen, W. R. Giles, and C. Ficet, "T-tubule localization of the inward-rectifier K^+ channel in mouse ventricular myocytes: a role in K^+ accumulation," *J. Physiol.,* vol. 537, pp. 979-992, Dec. 2001.

[18] M. C. Olsson, B. M. Palmer, B. L. Stauffer, L. A. Leinwand, and R. L. Moore, "Morphological and functional alterations in ventricular myocytes from male transgenic mice with hypertrophic cardiomyopathy," *Circ. Res.,* vol. 94, pp. 201-207, Feb. 2004.

[19] H. V. M. van Rijen, D. Eckardt, J. Degen, M. Theis, T. Ott, K. Willecke, H. J. Jongsma, T. Opthof, and J. M. T. de Bakker, "Slow conduction and enhanced anisotropy increase the propensity for ventricular tachyarrhythmias in adult mice with induced deletion of connexin43," *Circulation,* vol. 109, pp. 1048-1055, Mar. 2004.

[20] S. Bagwe, O. Berenfeld, D. Vaidya, G. E. Morley, and J. Jalife, "Altered right atrial excitation and propagation in connexin40 knockout mice," *Circulation,* vol. 112, pp. 2245-2253, Oct. 2005.

[21] H. V. Huikuri, A. Castellanos, and R. J. Myerburg, "Sudden death due to cardiac arrhythmias," *N. Engl. J. Med.,* vol. 345, pp. 1473-1482, Nov. 2001.

[22] M. E. Curran, I. Splawski, K. W. Timothy, G. M. Vincent, E. D. Green, and M. T. Keating, "A molecular basis for cardiac arrhythmia: *HERG* mutations cause long QT syndrome," *Cell,* vol. 80, pp. 795-803, Mar. 1995.

[23] M. C. Sanguinetti, C. Jiang, M. E. Curran, and M. T. Keating, "A mechanistic link between an inherited and an acquired cardiac arrhythmia: *HERG* encodes the I_{Kr} potassium channel," *Cell,* vol. 81, pp. 299-307, Apr. 1995.

[24] N. Wiener and A. Rosenbluth, "The mathematical formulation of the problem of conduction of impulses in a network of connected excitable elements, specifically in cardiac muscle," *Arch. Inst. Cardiol. Mexico,* vol. 16, pp. 205-265, 1946.

[25] G. K. Moe, W. C. Rheinboldt, and J. A. Abildskov, "A computer model of atrial fibrillation," *Am. Heart. J.,* vol. 67, pp. 200-220, Feb. 1964.

[26] V. I. Krinskii, "Excitation propagation in nonhomogenous medium (actions analogous to heart fibrillation)," *Biofizika,* vol. 11, pp. 676-683, Jul.-Aug. 1966.

[27] V. I. Krinsky, "Mathematical models of cardiac arrhythmias (spiral waves)," *Pharmacol. Ther. B,* vol. 3, pp. 539-555, 1978.

[28] F. J. van Capelle and D. Durrer, "Computer simulation of arrhythmias in a network of coupled excitable elements," *Circ. Res.,* vol. 47, pp. 454-466, Sep. 1980.

[29] A. T. Winfree, "Electrical instability in cardiac muscle: phase singularities and rotors," *J. Theor. Biol.,* vol. 138, pp. 353-405, Jun. 1989.

[30] A. M. Pertsov, J. M. Davidenko, R. Salomonsz, W. T. Baxter, and J. Jalife, "Spiral waves of excitation underlie reentrant activity in isolated cardiac muscle," *Circ. Res.,* vol. 72, pp. 631-650, Mar. 1993.

[31] J. J. Fox, M. L. Riccio, F. Hua, E. Bodenschatz, and R. F. Gilmour, Jr., "Spatiotemporal transition to conduction block in canine ventricle," *Circ. Res.,* vol. 90, pp. 289-296, Feb. 2002.

[32] J. Jalife and O. Berenfeld, "Molecular mechanisms and global dynamics of fibrillation: an integrative approach to the underlying basis of vortex-like reentry," *J. Theor. Biol.,* vol. 230, pp. 475-487, Oct. 2004.

[33] A. G. Kleber and Y. Rudy, "Basic mechanisms of cardiac impulse propagation and associated arrhythmias," *Physiol. Rev.,* vol. 84, pp. 431-488, Apr. 2004.

[34] Z. Qu, H. S. Karagueuzian, A. Garfinkel, J. N. Weiss, "Effects of Na^+ channel and cell coupling abnormalities on vulnerability to reentry: a

simulation study," *Am. J. Physiol.,* vol. 286, pp. H1310-H1321, Apr. 2004.
[35] P. Comtois, J. Kneller, and S. Nattel, "Of circles and spirals: bridging the gap between the leading circle and spiral wave concepts of cardiac reentry," *Europace,* vol. 7 (Suppl 2), pp. 10-20, Sep. 2005.
[36] J. N. Weiss, A. Karma, Y. Shiferaw, P. S. Chen, A. Garfinkel, and Z. Qu, "From pulsus to pulseless: the saga of cardiac alternans," *Circ. Res.,* vol. 98, pp. 1244-1253, May 2006.
[37] S. W. Morgan, G. Plank, I. V. Biktasheva, and V. N. Biktashev, "Low energy defibrillation in human cardiac tissue: a simulation study," *Biophys. J.,* vol. 96, pp. 1364-1373, Feb. 2009.
[38] J. M. Davidenko, P. F. Kent, D. R. Chialvo, D. C. Michaels, and J. Jalife, "Sustained vortex-like waves in normal isolated ventricular muscle," *Proc. Natl. Acad. Sci. USA,* vol. 87, pp. 8785-8789, Nov. 1990.
[39] J. M. Davidenko, A. V. Pertsov, R. Salomonsz, W. Baxter, and J. Jalife, "Stationary and drifting spiral waves of excitation in isolated cardiac muscle," *Nature,* vol. 355, pp. 349-351, Jan. 1992.
[40] P. S. Chen, A. Garfinkel, J. N. Weiss, and H. S. Karagueuzian, "Spirals, chaos, and new mechanisms of wave propagation," *Pacing Clin. Electrophysiol.,* vol. 20, pp. 414-421, Feb. 1997.
[41] A. Garfinkel, P. S. Chen, D. O. Walter, H. S. Karagueuzian, B. Kogan, S. J. Evans, M. Karpoukhin, C. Hwang, T. Uchida, M. Gotoh, O. Nwasokwa, P. Sager, and J. N. Weiss, "Quasiperiodicity and chaos in cardiac fibrillation," *J. Clin. Invest.,* vol. 99, pp. 305-314, Jan. 1997.
[42] Y. H. Kim, A. Garfinkel, T. Ikeda, T. J. Wu, C. A. Athill, J. N. Weiss, H. S. Karagueuzian, and P. S. Chen, "Spatiotemporal complexity of ventricular fibrillation revealed by tissue mass reduction in isolated swine right ventricle: further evidence for the quasiperiodic route to chaos hypothesis," *J. Clin. Invest.,* vol. 100, pp. 2486-2500, Nov. 1997.
[43] R. A. Gray, A. M. Pertsov, and J. Jalife, "Spatial and temporal organization during cardiac fibrillation," *Nature,* vol. 392, pp. 75-78, Mar. 1998.
[44] F. X. Witkowski, L. J. Leon, P. A. Penkoske, W. R. Giles, M. L. Spano, W. L. Ditto, and A. T. Winfree, "Spatiotemporal evolution of ventricular fibrillation," *Nature,* vol. 392, pp. 78-82, Mar. 1998.
[45] R. F. Gilmour, Jr., "Electrical restitution and ventricular fibrillation: negotiating a slippery slope," *J. Cardiovasc. Electrophysiol.,* vol. 13, pp. 1150-1151, Nov. 2002.
[46] J. N. Weiss, Z. Qu, P. S. Chen, S. F. Lin, H. S. Karagueuzian, H. Hayashi, A. Garfinkel, and A. Karma, "The dynamics of cardiac fibrillation," *Circulation,* vol. 112, pp. 1232-1240, Aug. 2005.
[47] A. Palmer, J. Brindley, and A. V. Holden, "Initiation and stability of reentry in two coupled excitable fibers," *Bull. Math. Biol.,* vol. 54, pp. 1039-1056, Nov. 1992.
[48] J. M. Rogers and A. D. McCulloch, "A collocation-Galerkin finite element model of cardiac action potential propagation," *IEEE Trans. Biomed. Eng.,* vol. 41, pp. 743-757, Aug. 1994.
[49] J. M. Davidenko, R. Salomonsz, A. M. Pertsov, W. T. Baxter, and J. Jalife, "Effects of pacing on stationary reentrant activity: theoretical and experimental study," *Circ. Res.,* vol. 77, pp. 1166-1179, Dec. 1995.
[50] C. F. Starmer, D. N. Romashko, R. S. Reddy, Y. I. Zilberter, J. Starobin, A. O. Grant, and V. I. Krinsky, "Proarrhythmic response to potassium channel blockade: numerical studies of polymorphic tachyarrhythmias," *Circulation,* vol. 92, pp. 595-605, Aug. 1995.
[51] P. S. Chen, P. D. Wolf, E. G. Dixon, N. D. Danieley, D. W. Frazier, W. M. Smith, and R. E. Ideker, "Mechanism of ventricular vulnerability to single premature stimuli in open-chest dogs," *Circ. Res.,* vol. 62, pp. 1191-1209, Jun. 1988.
[52] N. Shibata, P. S. Chen, E. G. Dixon, P. D. Wolf, N. D. Danieley, W. M. Smith, and R. E. Ideker, "Influence of shock strength and timing on induction of ventricular arrhythmias in dogs," *Am. J. Physiol.,* vol. 255, pp. H891-H901, Oct. 1988.
[53] D. W. Frazier, P. D. Wolf, J. M. Wharton, A. S. Tang, W. M. Smith, and R. E. Ideker, "Stimulus-induced critical point. Mechanism for electrical initiation of reentry in normal canine myocardium," *J. Clin. Invest.,* vol. 83, pp. 1039-1052, Mar. 1989.
[54] G. P. Walcott, S. B. Knisley, X. Zhou, J. C. Newton, and R. E. Ideker, "On the mechanism of ventricular defibrillation," *Pacing Clin. Electrophysiol.,* vol. 20, pp. 422-431, Feb. 1997.
[55] S. F. Noujaim, S. V. Pandit, O. Berenfeld, K. Vikstrom, M. Cerrone, S. Mironov, M. Zugermayr, A. N. Lopatin, and J. Jalife, "Up-regulation of the inward rectifier K^+ current (I_{K1}) in the mouse heart accelerates and stabilizes rotors," *J. Physiol.,* vol. 578, pp. 315-326, Jan. 2007.
[56] W. Guo, H. Li, B. London, and J. M. Nerbonne, "Functional consequences of elimination of $I_{to,f}$ and $I_{to,s}$: early afterdepolarizations, atrioventricular block, and ventricular arrhythmias in mice lacking Kv1.4 and expressing a dominant-negative Kv4 α subunit," *Circ. Res.,* vol. 87, pp. 73-79, Jul. 2000.

Vladimir E. Bondarenko graduated from Faculty of Physics, Moscow State University (Moscow, Russia) in 1986. In 1990 he obtained a degree Candidate of Science in Physics and Mathematics (PhD analog) from Faculty of Physics, Moscow State University (Moscow, Russia). His major fields of study are plasma physics, polymer science, dynamical systems, ion channel models, neural network models, cardiac cellular and multicellular models.

Since graduation in 1986 from Moscow State University, he worked as an Engineer, Junior Researcher, and Researcher in A. L. Mintz Radiotechnical Institute, Moscow, Russia ('86-'94), Researcher and Senior Researcher in the Institute of Biochemical Physics, Moscow, Russia ('94-'98), Postdoctoral Fellow in the University of Pittsburgh, Pittsburgh, PA ('98-'99) and Penn State University, Hershey, PA ('99-'00), Postdoctoral Fellow and Research Assistant Professor in the University of Buffalo, SUNY, Buffalo, NY ('00-'08). Currently he is an Assistant Professor in the Department of Mathematics and Statistics, Georgia State University, Atlanta, GA. He has published more than 40 papers in peer reviewed journals and a number of papers in conference proceedings. Current research interests include ion channels, neural and cardiac cell models, and models of cardiac arrhythmias.

Dr. Bondarenko is a member of Biophysical Society and American Physical Society.

Randall L. Rasmusson (M '88) Graduated from Rice University Houston TX with a BS in electrical engineering and computer science in 1983 and an MS in electrical engineering in 1986. He received a Ph.D. in physiology from Duke University, Durham, N.C. in 1991.

He served as a Research Assistant Professor at Duke University Department of Biomedical Engineering ('91-'97), Assistant Professor at MCP Hahnemann University ('97-'99), Associate Professor at Pennsylvania State University, Department of Physiology ('99-'00) and Associate Professor ('00-'06) or Professor at SUNY Buffalo, Department of Physiology and Biophysics, Buffalo NY ('06-present). He has published over 70 research articles, reviews, and book chapters. His research interests are understanding ion channel biophysics and integrative modeling of abnormal cellular electrical behavior during arrhythmias and in autism.

Dr. Rasmusson is an Established Investigator and Fellow of the American Heart Association. He is a member of the Biophysical Society, the Biomedical Engineering Society, The Physiological Society and the American Physiological Society.